Freestream Turbulence Effects on Stagnation Point Heat Transfer

R.M. Traci* and D.C. Wilcox†
Science Applications, Inc., El Segundo, Calif.

Freestream turbulence effects on stagnation-point flow have been studied analytically, with particular emphasis on the resulting augmentation of wall heat transfer. Calculations are based on the Saffman-turbulence-model equations. Three distinct flow regimes have received study: 1) the uniform mean flow far from the stagnation point; 2) an inviscid mean flow region with constant rate of strain connecting region 1 to region 3; and 3) the wall region in which viscous effects appear. The overall solution is achieved by analytical/numerical solution matching. Results have been compiled for turbulence structure and wall heat transfer, including comparisons with corresponding low-speed experimental data.

I. Introduction

LAMINAR-stagnation-point flow (Hiemenz flow) is one of the few flows for which an exact solution to the Navier-Stokes equations[1] is easily obtained and, for this reason, in addition to its practical importance, has been the subject of many classical studies. Froessling[2] and Squire[3] for example, present theories for stagnation-point heat transfer for incompressible flow which have been extended to include compressibility and real gas effects by a number of investigators, most notably by Fay and Riddell.[4]

Early experimental studies of stagnation-point heat transfer for low-speed flows indicated that theories consistently underpredicted stagnation-point heat transfer. Freestream turbulence effects were found to be the causes of the discrepancy, and further experimental work by Kestin[5,6], Smith and Kuethe,[7] Zapp[8] and others demonstrated the dramatic effect of freestream turbulence intensity Θ $(Re_D)^{1/2}$ where Re_D is Reynolds number based on body diameter and freestream flow conditions. This was the governing parameter in their semiempirical analysis of turbulent stagnation point flow, an analysis based on an assumed form (with an empirical constant) for the turbulent eddy viscosity in the boundary layer. Based on their data, they also postulated a Reynolds-number dependence, but gave no physical justification for the postulated dependence.

Early theoretical investigations[9-11] predicted that freestream oscillations would have little or no effect on mean boundary-layer heat transfer or shear stress. This conclusion was confirmed by Ishigaki[12] who thoroughly studied effects of freestream oscillations of various frequencies on stagnation-point flow. An alternate theoretical approach was taken by Sutera, Maeder, and Kestin[13] and Sutera[14] who showed that the introduction of vorticity in the freestream resulted in substantial increases in stagnation-point heat transfer. They identified the mechanism as stretching (amplification) of vortex lines in the divergent stagnation point flow. Sadeh, Sutera, and Maeder[15] extended the vorticity-amplification theory to include a treatment of the flow outside the boundary layer extending to the freestream. They provided further delineation of the importance of wavelength (scale) on the degree of amplification. In a complementary experimental study, Sadeh et al.[16] presented turbulence measurements which demonstrated good agreements with trends predicted by the theory. These studies resulted in a good understanding of the flow mechanisms involved in the freestream turbulence problem, but they fail to provide a capability for quantitative predictions.

In the present study, the stagnation-point flow of a turbulent medium is analyzed by making use of recent progress in turbulence modeling to describe the nature and evolution of the turbulent structure in a stagnation region. The Saffman turbulence model[17-19] is used, as it offers promise of accounting for both turbulence intensity and scale in a straightforward manner. The model possesses sufficiently generality to make a priori predictions of freestream turbulence effects; that is, no empirical information about the solution is required. The Saffman model has been applied with success in prior analyses to describe a wide range of complicated turbulent flow phenomena such as flow with a strong pressure gradient[18], wall roughness effects,[19] and boundary-layer separation[20] and transition.[21]

The problem is formulated in Sec. II, where the coupled set of time-averaged Navier-Stokes equations and turbulence-model equations is demonstrated to be reducible to a closed set of ordinary differential equations near a stagnation point. Three important and distinct flow regions are identified, and a method is described which involves matching of the solutions in each region. Section III presents theoretical results for a circular cylinder; these results delineate the effect of turbulence intensity and scale as well as flow Reynolds number on stagnation-point heat transfer and shear stress. Theoretical results are compared with corresponding experimental data. The final section summarizes results and conclusions.

II. Formulation and Solution Procedure

A. Governing Equations

Based on the time-averaged Navier-Stokes equations and Saffman turbulence model, stagnation-point flow of a turbulent fluid is formulated in this section. Figure 1 schematically represents the flowfield. As indicated, the stagnation point is taken as the coordinate-system origin; x and y denote distance parallel to and normal to the surface, respectively, with corresponding velocity components u and v. Steady flow of an incompressible, constant-property fluid is considered. The equations of motion used are the time-averaged conservation equations, which for two-dimensional ($n=0$) and axisymmetric ($n=1$) flow are

Presented as Paper 74-515 at the AIAA 7th Fluid and Plasma Dynamics Conference, Palo Alto, California, June 17-19, 1974; submitted July 15, 1974; revision received December 16, 1974.

Index category: Boundary Layers and Convective Heat Transfer—Turbulent.

*Staff Scientist. Currently with DCW Industries, Sherman Oaks, Calif. Member AIAA.

†Consultant; also Owner, DCW Industries, Sherman Oaks, Calif. Member AIAA.

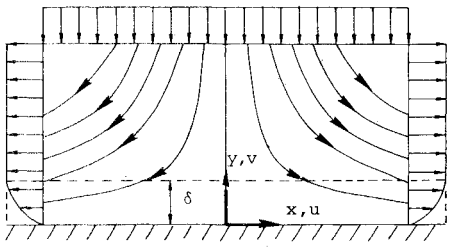

Fig. 1 Schematic of stagnation-point flowfield.

$$(1/x^n)(\partial/\partial x)(x^n u)+\partial v/\partial y=0 \tag{1}$$

$$u(\partial u/\partial x)+v(\partial u/\partial y)=-(1/\rho)\ (\partial p/\partial x)+(1/x^n)(\partial/\partial x)\ (x^n\tau_{xx})+\partial\tau_{xy}/\partial y-n\tau_{\theta\theta}/x \tag{2}$$

$$u(\partial v/\partial x)+v(\partial v/\partial y)=-(1/\rho)\ (\partial p/\partial y)+(1/x^n)(\partial/\partial x)\ (x^n\tau_{xy})+\partial\tau_{yy}/\partial y \tag{3}$$

$$u(\partial t/\partial x)+v(\partial t/\partial y)=-(1/x^n)(\partial/\partial x)(x^n q_x)-(\partial q_y/\partial y)+\phi \tag{4}$$

where p, ρ, and t signify mean pressure, density, and temperature, respectively. The sum of laminar and Reynolds stress tensors is denoted by τ_{ij}, and q_i is the heat-flux vector. For brevity the viscous dissipation function ϕ in the mean-flow energy equation [Eq. (4)] is not written in detail; it is negligible (see Sec. IIB).

Closure of the above system of equations is achieved by using the Saffman turbulence model to relate the Reynolds stresses and turbulent heat-flux vector to mean flow properties. An eddy viscosity ϵ is used to relate the total stress τ_{ij} to the mean rate of strain tensor S_{ij} as follows:

$$\tau_{ij}=2(\nu+\epsilon)S_{ij}-\tfrac{2}{3}e\delta_{ij} \tag{5}$$

where ν is kinematic viscosity, e is specific turbulent energy, and δ_{ij} is the Kronecker delta. Similarly, an eddy conductivity, which is related to the eddy viscosity through a turbulent Prandtl number, is used to relate the turbulent contribution of the heat flux vector to the mean temperature gradient. Thus the combined molecular and turbulent heat flux vector is given by

$$q_i=-(\nu/Pr_L+\epsilon/Pr_T)\partial t/\partial x_i \tag{6}$$

where Pr_L and Pr_T are the laminar and turbulent Prandtl numbers, respectively.

In the Saffman model, eddy viscosity is calculated as the ratio of the turbulent energy e to a turbulent dissipation rate (pseudovorticity) ω, i.e.,

$$\epsilon=e/\omega \tag{7}$$

where e and ω satisfy the following equations:

$$u(\partial e/\partial x)+v(\partial e/\partial y)=\alpha^* e\{2(\partial u/\partial x)^2+2n(u/x)^2+2(\partial v/\partial y)^2+(\partial u/\partial y+\partial v/\partial x)^2\}^{1/2}-\beta^*\omega e+(1/x^n)(\partial/\partial x)\{x^n(\nu+\sigma^*\epsilon)\partial e/\partial x\}+(\partial/\partial y)\{(\nu+\sigma^*\epsilon)\partial e/\partial y\} \tag{8}$$

$$u(\partial\omega^2/\partial x)+v(\partial\omega^2/\partial y)=\alpha\omega^2\{(\partial u/\partial x)^2+n(u/x)^2+(\partial u/\partial y)^2+(\partial v/\partial x)^2+(\partial v/\partial y)^2\}^{1/2}-\beta\omega^3+(1/x^n)(\partial/\partial x)\{x^n(\nu+\sigma\epsilon)\partial\omega^2/\partial x\}+(\partial/\partial y)\{(\nu+\sigma\epsilon)\partial\omega^2/\partial y\} \tag{9}$$

where α, β, σ, α^*, β^*, σ^*, are constants in the model equations. Values for these constants have been established in previous analyses from general arguments and their values are

$$\alpha=0.2638,\ \beta=0.18,\ \sigma=0.50$$
$$\alpha^*=0.30,\ \beta^*=0.09,\ \sigma^*=0.50 \tag{10}$$

The formulation is completed by boundary conditions at the wall ($y=0$) and in the inviscid freestream ($y\to\infty$) for the governing equations [Eqs. (1-4) and (7-10)]. Conditions on the mean flow quantities are defined in the usual way by prescribing wall temperature, t_w, and the no-slip velocity boundary condition at $y=0$. Conditions on the turbulence quantities e and ω for a perfect smooth wall, as devised by Saffman and Wilcox, are

$$\left.\begin{aligned} e&=0\\ y^2\omega&=20\nu/\beta\end{aligned}\right\}\quad \text{at } y=0 \tag{11}$$

Finally, all flow and turbulence quantities are required to match their prescribed freestream values as $y\to\infty$. The definition and prescription of "freestream" quantities form an important part of the present analysis and will be discussed in detail below.

B. Transformation of Equations

The governing equations can be reduced to a closed set of ordinary differential equations in the vicinity of a stagnation point. First, note that the turbulent fluctuations and the mean flow couple strongly only in a thin viscous region near the wall. Outside this region, the turbulent fluctuations are too small to distort the inviscid mean flow about the body whose stagnation point is being considered. Thus the mean flow outside the viscous region satisfies the usual inviscid solution near a stagnation point given by

$$u=cx,\ v=-(n+1)cy \tag{12}$$

where $c=\partial u/\partial x$ is the inviscid flow velocity gradient which depends on the shape of the body under consideration, as well as on freestream flow properties.

Following the lead of the laminar stagnation-point solution, the following transformation is introduced in the viscous region:

$$\eta=(c/\nu)^{1/2}y,\ \xi=(c/\nu)^{1/2}x \tag{13}$$

and a solution of the following form is sought:

$$u=(\nu c)^{1/2}\xi U(\eta) \tag{14a}$$
$$v=(\nu c)^{1/2}V(\eta) \tag{14b}$$
$$t=t_w+(t_\infty-t_w)T(\eta) \tag{14c}$$
$$p_0-p=\rho c\nu\{F(\eta)+\xi^2/2\} \tag{14d}$$
$$e=\nu cE(\eta) \tag{14e}$$
$$\omega=cW(\eta) \tag{14f}$$

where t_∞, t_w are mean flow temperatures far from the wall and at the wall, respectively, and p_0 is the stagnation pressure. This transformation, along with two minor simplifying approximations, is sufficient to reduce the equations of motion to ordinary differential equations.

The first approximation concerns the viscous dissipation in the mean flow energy equation, which, near the stagnation point, can be shown to be of the order of an Eckert number, i.e.,

$$\phi_{ND}\sim Pr_L\nu c\xi^2/C_p(t_0-t_w) \tag{15}$$

where C_p is specific heat, t_0 is total temperature, and the subscript ND denotes nondimensionalization. Note that $\phi\to 0$ very rapidly as $\xi\to 0$ so that ϕ can be neglected near the stagnation point. Experience shows that this is a very good approximation near the stagnation point even in high-speed flows.

The second approximation concerns the so-called "production" terms in the turbulence-model equations. For example, in the turbulent energy equation, the nondimensional production term is

$$\alpha^*\{4(2n+1)U^2+\xi^2(dU/d\eta)^2\}^{1/2}E$$
$$\doteq \alpha^* 2(2n+1)^{1/2}|U|E+O(\xi^2) \tag{16}$$

and similarly for the dissipation-rate equation. Again, the $O(\xi^2)$ terms are small very near the stagnation point ($\xi \mapsto 0$) and are therefore neglected.

Using the transformation given by Eqs. (13) and (14) and these two approximations permits reduction of the equations of motion to the following set of ordinary differential equations:

$$dV/d\eta+(n+1)U=0 \tag{17}$$

$$(d/d\eta)(VU)=1-(n+2)U^2+(d/d\eta)\{(1+E/W)dU/d\eta\} \tag{18}$$

$$dF/d\eta=(d/d\eta)\{V^2/2+2(n+1)(1+E/W)U+E/3\}$$
$$-(n+1)(1+E/W)dU/d\eta \tag{19}$$

$$(d/d\eta)(VT)=-(n+1)UT+(d/d\eta)$$
$$\{(1/Pr_L+E/WPr_T)dT/d\eta\} \tag{20}$$

$$(d/d\eta)(VE)=\{2(2n+1)^{1/2}\alpha^*|U|-(n+1)U\}E-\beta^*WE$$
$$+(d/d\eta)\{(1+\sigma^*E/W)dE/D\eta\} \tag{21}$$

$$(d/d\eta)(VW^2)=\{(2(2n+1)^{1/2}\alpha|U|-(n+1)U\}W^2-\beta W^3$$
$$+(d/d\eta)\{(1+\sigma E/W)dW^2/d\eta\} \tag{22}$$

In terms of the similarity formulation, the wall boundary conditions become

$$U=V=T=F=0$$
$$E=0,\ \eta^2W=20/\beta \qquad \text{at } \eta=0 \tag{23}$$

Away from the surface the solution must asymptotically approach the freestream conditions so that

$$\left.\begin{aligned} &U(\eta)\to 1, \quad T(\eta)\to 1\\ &E(\eta)\to e_\infty/\nu c, \quad W(\eta)\to \omega_\infty/c\end{aligned}\right\} \quad \text{as } \eta\to\infty \tag{24}$$

Note that the equations describing the nondimensional pressure, $F(\eta)$ [Eq. (19)], and the mean flow temperature, $T(\eta)$ [Eq. (20)], uncouple from the rest of the equations and therefore can be solved by quadrature. Specifically,

$$F(\eta)=V^2(\eta)/2+2(n+1)[(1+E/W)U(\eta)]+E(\eta)/3$$
$$+(n+1)\int_0^\eta (1+E/W)(dU/d\eta)d\eta \tag{25}$$

$$T(\eta)=Q_w\int_0^\eta (1/Pr_L+E/WPr_T)^{-1}\exp$$
$$\{\int_0^{\eta'} V(\tilde{\eta})(1/Pr_L+E/WPr_T)^{-1}d\tilde{\eta}\}d\eta' \tag{26}$$

where Q_w is the nondimensional heat flux from the fluid to the surface given by

$$Q_w=\left[\int_0^\infty (1/Pr_L+E/WPr_T)^{-1}\exp\right.$$
$$\left.\times\{\int_0^{\eta'} V(\tilde{\eta})\,(1/Pr_L+E/WPr_T)^{-1}d\tilde{\eta}\}d\eta'\right]^{-1} \tag{27}$$

Hence, the nonlinear problem becomes one of solving the seventh-order set of coupled ordinary differential equations, Eqs. (17, 18, 21, and 22), subject to the boundary conditions on $U(\eta)$, $V(\eta)$, $E(\eta)$, and $W(\eta)$ given in Eqs. (23) and (24). Since boundary conditions are posed at two locations, two-point boundary-value problem solution techniques are required. The solution method, which involves matching of solutions in separate flow regions between the freestream and the body, is presented in the next section.

C. Solution Methodology: Identification and Analysis of Three Flow Regions

Analysis of the previously mentioned boundary value problem includes investigation of the following three distinct flow regimes (see Fig. 2). Region 1: freestream flow consisting of a uniform mean flow away from any influence of the solid surface (cylinder, sphere, etc.). Region 2: body distorted flow consisting of an inviscid mean flow with strain. Region 3: viscous, wall-region flow dominated by the no-slip boundary condition at the stagnation surface. Rationale for considering the three regions and an analysis of their mean flow and turbulence structure are now presented.

Region 1

On the one hand, the formulation presented above requires the prescription of both the turbulent energy e and the dissipation rate ω in the freestream ($y\to\infty$). On the other hand, in experimental studies, turbulence is introduced into a uniform stream by passage through a grid and is generally characterized at the test section solely by a measured rms velocity fluctuation (turbulent energy). In order to compare the present results with available data, the appropriate value for freestream dissipation rate (or equivalently the length scale of the turbulence) must also be defined. This is accomplished by using the model equations to analyze grid turbulence in the freestream.

Considering first the freestream value of e, note that wind-tunnel studies traditionally define freestream turbulence intensity (Θ) as the ratio of rms streamwise velocity fluctuation to freestream velocity. This convention is followed here; assuming the grid turbulence isotropic, Θ is related to the turbulent energy in the following manner:

$$\Theta=\langle v'^2\rangle^{1/2}/V_\infty=(\tfrac{2}{3}e_\infty)^{1/2}/V_\infty \tag{28}$$

where V_∞ is freestream velocity, prime denotes the fluctuating velocity component, and $\langle\ \rangle$ denotes time average. Values of Θ are readily available from the various wind-tunnel studies considered herein.

Turning now to the freestream dissipation rate, note that the freestream solution to the model equations is

$$e/e_0=\omega/\omega_0=[1+\beta\omega_0(y_0-y)/2V_\infty]^{-1} \tag{29}$$

where subscript o denotes conditions at a point $y=y_o$ in the freestream. A turbulent length scale, ℓ can be defined[17] from e and ω as

$$\ell=e^{1/2}/\alpha^*\omega \tag{30}$$

so that

$$\ell/\ell_o=[1+\beta\omega_0(y_0-y)/2V_\infty]^{1/2} \tag{31}$$

Equations (29) and (31) define the variation of turbulence properties at all points in the freestream once the reference quantities e_0, ω_0, and y_0 are determined. Smith and Kuethe[7] present sufficient data on the decay of the rms streamwise velocity fluctuation, and hence the decay of e, as a function of y to fix the values of y_0 and ω_0. That is, ω_0 and y_0 are determined by fitting the Smith and Kuethe data with Eq. (29). Thus, for any intensity e_∞, corresponding values of ω_∞ or, equivalently, ℓ_∞, can be determined from Eqs. (29) and (31) for the Smith and Kuethe data. For the purpose of this study, freestream turbulence is completely characterized by the length scale, ℓ, and the intensity, Θ, and all results of the next section will be presented in terms of these parameters rather than the model parameters e and ω.

Region 2

To a good approximation, Region 2 is an inviscid flow region with strain in which the Reynolds stresses do not affect the mean flow. The mean rate of strain, however, has a significant effect on the turbulence structure which must be modeled in order to couple the wall region to the freestream. The flow in this region is modeled as a flow experiencing a constant rate of strain; the turbulence model equations are solved to determine the variation of turbulent energy and dissipation rate as the fluid approaches the stagnation region. A first approximation to the mean velocity field in this region (in terms of the scaled variables introduced above) is given by

$$U(\eta)=1,\ V(\eta)=-(n+1)\eta \tag{32}$$

For simplicity, the velocity distribution on the stagnation streamline is approximated as a straight-line extrapolation of the inviscid stagnation point solution out to the freestream. To this approximation, the location of the undisturbed freestream flow, in terms of the scaled normal coordinate, is

$$\eta_\infty = V_\infty/(n+1)(\nu c)^{1/2} \tag{33}$$

Equation (33) defines the coordinate location for applying the freestream conditions on e and ω.

For the mean velocity field given in Eq. (31), the equations for e and ω are

$$-(n+1)\eta dE/d\eta = (2(2n+1)^{1/2}\alpha^* - \beta^* W)E + (d/d\eta)[(\sigma^* E/W)dE/d\eta] \tag{34}$$

$$-(n+1)\eta dW^2/d\eta = ((2(2n+1))^{1/2}\alpha - \beta W)W^2 + (d/d\eta)[(\sigma E/W)dW^2/d\eta] \tag{35}$$

These equations account for the production, dissipation and diffusion of turbulent energy in a region of constant mean rate of strain. The boundary (initial) conditions are defined at η_∞ by the freestream conditions (e_∞, ω_∞) plus conditions on the gradients which arise from neglecting diffusion at η_∞. The boundary conditions are

$$\left.\begin{aligned} &E = e_\infty/\nu c,\ W = \omega_\infty/c \\ &dE/d\eta = E(\beta^* W - 2(2n+1)^{1/2}\alpha^*)/(n+1)\eta_\infty \\ &dW/d\eta = W(\beta W - [2(2n+1)]^{1/2}\alpha)/2(n+1)\eta \end{aligned}\right\} \text{ at } \eta=\eta_\infty \tag{36}$$

The initial value problem defined by Eqs. (34-36) could be solved most directly by using a standard numerical integration scheme to integrate from η_∞ toward the wall, starting with the appropriate initial values [Eq. (36).] Unfortunately, it can be demonstrated both analytically and numerically that the equations admit divergent solutions when integrated toward the wall so that small errors in the starting values grow rapidly and destroy the solution. Thus the solution has been accomplished by using a shooting method whereby guesses are made for E and W at an arbitrary value of $\eta(\eta_I$ in Fig. 2) which defines the outer boundary of the viscous wall region (Region 3). The equations are integrated from η_I to η_∞ using a standard Adams-Moulton predicter-corrector numerical scheme. New guesses are then made for the conditions at η_I until the resulting values of E and W at η_∞ are equal to the desired values $E(\eta_\infty)$ and $W(\eta_\infty)$ within some arbitrary small error (taken as one percent).

Figure 3 shows a typical solution for the variation of turbulent energy approaching the stagnation surface. The important effect, demonstrated in the figure, is the amplification of turbulent energy in Region 2. For example, when $Re_D = 10^6$ and $(\ell/D)(Re_D)^{1/2} = 10$, the turbulent energy will be amplified by a factor of almost three as the fluid moves from the freestream to the edge of the viscous region; by contrast, when $Re_D = 10^4$ and $(\ell/D)(Re_D)^{1/2} = 10$, the turbulent energy is

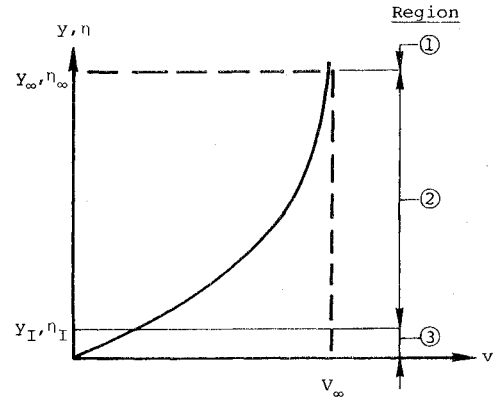

Fig. 2 Schematic of mean velocity approaching a stagnation point.

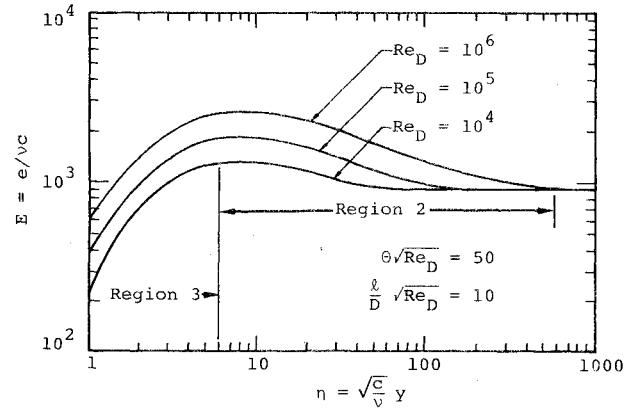

Fig. 3 Variation of turbulent energy approaching the stagnation point.

increased by about 35%. The significant amplification shown is consistent with the experimental measurements of Bearman[22] and Sadeh et al.[16] concerning the behavior of small-scale turbulence approaching a two-dimensional bluff body. Specifically, Sadeh finds that e is amplified by a factor of between 2 and 3 for $Re_D = 2.5\times10^5$ and $65 < \Theta(Re_D)^{1/2} < 120$.

Bearman and Sadeh both identify the amplification mechanism as vortex stretching due to the strain in the mean flowfield in the manner of the "vorticity amplification" theory[13,15] just mentioned. Vortex stretching, viewed in the context of the Saffman model, shows up in the turbulent energy production term which is proportional to the mean strain rate. Hence the Saffman model appears consistent with the vorticity amplification hypothesis. As shown in Fig. 3, increasing η_∞ enhances turbulent energy amplification; this enhancement is due to the longer "time" that the mean rate of strain has to amplify the turbulence of a fluid particle as it approaches the stagnation point. This is identified as a freestream Reynolds number effect in Sec. III.

The solution for Region 2, obtained in the manner described above, provides the appropriate boundary conditions for the turbulence quantities (E_I, W_I) at $\eta=\eta_I$ as required for the solution of the viscous wall region.

Region 3

The region of most interest is the wall region ($0<\eta<\eta_I$), since the transport of momentum and energy to the wall are ultimately determined by the action of turbulence on the mean flow in this region. Due to the influence of the wall, the turbulence and mean flow are coupled. Therefore, the equations to be solved are the fully coupled equations in transformed form for U[Eq. (18)] and for the turbulence quantities E [Eq. (21)] and W [Eq. (22)], subject to the boundary condition at the wall [Eq. (23)] and at $\eta=\eta_I$ from the solution of

Region 2; also, note that $U=1$, $E=E_I$, and $W=W_I$ at $\eta=\eta_I$. Recall also that the other flow quantities (V,T,F) can be determined by suitable quadratures [Eqs. (25) and (26)] once the solutions for U, E, and W are obtained.

The two-point boundary value problem is solved by a time-marching finite-difference technique. That is, a second independent variable, t, is introduced and unsteady terms are added to the left-hand sides of the governing equations [$\partial U/\partial t$, $\partial E/\partial t$, and $\partial W^2/\partial t$ in Eqs. (18, 21, and 22), respectively]. The equations are integrated in time using an explicit time-marching one-dimensional finite difference scheme which uses a staggered mesh (after von Neumann-Richtmyer) and duFort-Frankel differencing for diffusion like terms. Starting from an initial guess, the solution evolves as the asymptotic limit of a time-varying field, i.e., as $\partial U/\partial t$, $\partial E/\partial t$, and $\partial W^2/\partial t$ become negligibly small. This approach to the solution of two-point boundary value problems obviates the complications encountered with standard shooting methods for such a high-order system of equations. The method has been used successfully in the present study and in similar applications in the past.[18]

As noted earlier, the choice of η_I which defines the outer boundary of the wall region is arbitrary. The value of η_I is based on two considerations: a) it must be large enough that the mean flow properties match the inviscid flow solution $U(\eta)=T(\eta)=1$ to good approximation; and b) it must be small enough to minimize numerical error and computational time (both related to finite-difference zone size). A good compromise of these conflicting requirements, which was used in all the calculations reported here, is $\eta_I=6$. Note that another value of η_I may be more appropriate for fluids other than air (the only fluid considered here) or for freestream turbulence parameters (E_∞, W_∞) out of the range of those considered in calculations performed to date.

III. Results and Comparison to Experiment

A. Parameterization

The effect of freestream turbulence on wall heat transfer and shear stress are of primary interest. Expressions for these quantities, with definition and examination of their parametric dependence, are now presented.

Based on the notation introduced, the heat transfer and shear stress at the wall are given by

$$q_w=k\partial t/\partial y=(\rho\mu)^{1/2}c^{1/2}C_p(t_\infty-t_w)\,Q_w(Pr_L,\ Pr_T,\ E_\infty,\ W_\infty,\ \eta_\infty) \tag{37}$$

and

$$\tau_w=\mu\partial u/\partial y=(\rho\mu)^{1/2}c^{3/2}xU_o'(E_\infty,\ W_\infty,\ \eta_\infty) \tag{38}$$

where μ and k are the molecular viscosity and conductivity, respectively, Q_w is given by Eq. (27), and U_0' is the derivative at the wall ($\eta=0$) of the scaled transverse velocity.

Equations (37) and (38) summarize the parametric dependence of heat transfer and shear stress on the relevant freestream turbulence parameters. These parameters can be presented in a more physical and recognizable form by relating them to a freestream turbulence intensity and length scale. This is accomplished by noting that the inviscid velocity gradient near a stagnation point, for bluff bodies of particular interest is given by

$$c=AV_\infty/D \tag{39}$$

where D is a typical body length scale (e.g., diameter) and A is a number depending upon body shape (from potential flow, $A=4$ for a cylinder and 3 for a sphere). Using this form for the inviscid flow velocity gradient, η_∞ [Eq. (33)] can be written

$$\eta_\infty=(Re_D/A)^{1/2}/(n+1) \tag{40}$$

where Re_D is the Reynolds number based on body diameter. Thus, freestream Reynolds number can affect the present results by increasing the extent (in scaled coordinates) of Region 2, which results in an increased amplification of turbulent energy in Region 2 as shown in Fig. 3.

Turbulence intensity and length scale are related to the turbulent energy and dissipation rate by Eqs. (28) and (30), respectively. Using the scaled form, E and W, and the relation for inviscid flow velocity gradient given in Eq. (39) leads to the natural nondimensional forms for turbulence intensity and scale,

$$\Theta(Re_D)^{1/2}=(\tfrac{2}{3}AE_\infty)^{1/2} \tag{41a}$$

and

$$\ell(Re_D)^{1/2}/D=(E_\infty/A)^{1/2}/\alpha^*W_\infty \tag{41b}$$

Also, defining a Nusselt number and shear stress coefficient in the usual manner

$$Nu_D=q_wD/k(t_\infty-t_w),\ c_f=2\tau_w/\rho V_\infty^2 \tag{42}$$

results in the following nondimensional forms for heat transfer and shear stress:

$$Nu_D/(Re_D)^{1/2}=\sqrt{A}Pr_LQ_w[\Theta(Re_D)^{1/2},\ \ell(Re_D)^{1/2}/D,\ Re_D,\ Pr_L,\ Pr_T] \tag{43}$$

and

$$c_f(Re_D)^{1/2}/(x/D)=2A^{3/2}\times U_0'[\Theta,\ (Re_D)^{1/2},\ \ell(Re_D)^{1/2}/D,\ Re_D] \tag{44}$$

Thus the present analysis includes the effect of three freestream parameters on the wall heat transfer in the form of a Froessling number, $[Nu_D/(Re_D)^{1/2}]$, viz, freestream turbulence intensity, $\Theta(Re_D)^{1/2}$, turbulence scale, $(\ell/D)(Re_D)^{1/2}$, and Reynolds number, Re_D. Previous authors have identified the effect of turbulence intensity but have only alluded to possible scale or Reynolds number effects. Effects of these parameters are now quantified for a circular cylinder in a low-speed crossflow.

B. Results for a Circular Cylinder in a Low-Speed Cross Flow

A considerable body of data exists for the effect of freestream turbulence on the stagnation-point heat transfer of a circular cylinder in a low-speed crossflow. The data are summarized in Fig. 4 and compared with this study's theoretical results. The theoretical results were calculated with $n=0$ (two-dimensional flow), $A=4$ (circular cylinder), and with the laminar and turbulent Prandtl numbers taken as 0.71 and 0.89 respectively. A turbulent Prandtl number of 0.89 was used, as it is the most appropriate value for boundary-layer flows.[1,17]

Figure 4 demonstrates the effect of the turbulence intensity parameter, $\Theta(Re_D)^{1/2}$, on heat transfer. Theoretical results are presented for three Reynolds numbers: $Re_D=10^4$, 10^5, 10^6 with a turbulence scale parameter, $(\ell/D)(Re_D)^{1/2}=10$. The values of Re_D chosen indicate the moderating effect of Reynolds number on heat transfer (Fig. 5) and effectively bracket the range of Reynolds numbers of the experimental data ($30{,}000<Re_D<240{,}000$). Note that the result for $Re_D=10^5$ provides an excellent fit to the data and, in fact, a Reynolds number of 10^5 is an appropriate "mean" value for the data. The turbulent scale parameter valid for most of the data can only be conjectured but should be similar to values which can be deduced from the Smith and Kuethe data.[7] Utilization of grid turbulence results (Sec. IIc) for the flow conditions and test geometry reported by Smith and Kuethe indicate that their data fall in the range of $5<(\ell/D)(Re_D)^{1/2}<30$. As will be shown (Fig. 6), turbulence scale has a minor effect (less than 5%) on the results for this range of $(\ell/D)(Re_D)^{1/2}$. Thus, the value used in the analytical calculations is

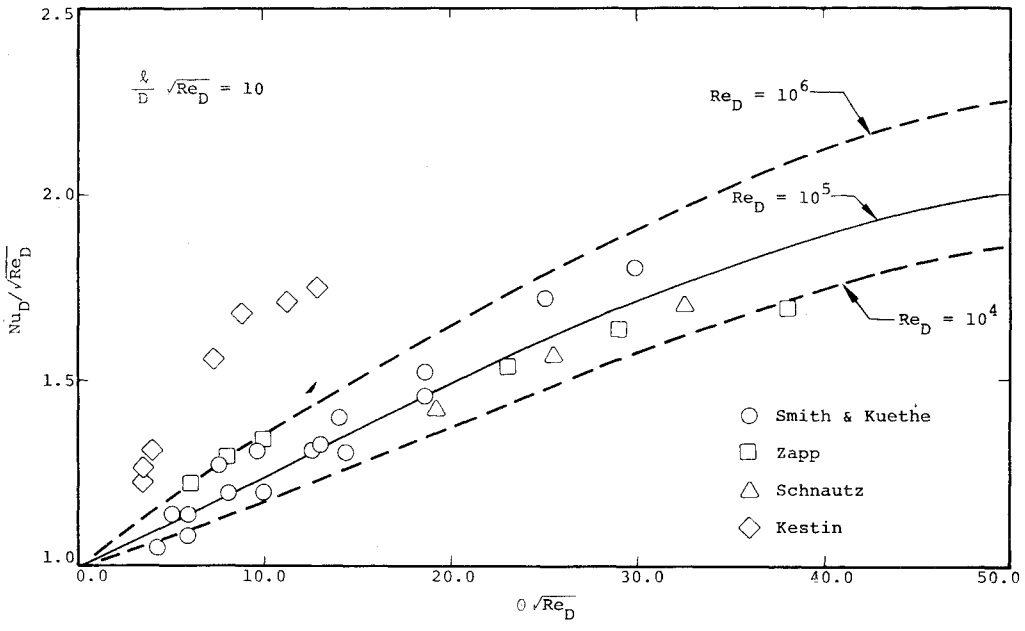

Fig. 4 Stagnation-point heat transfer to a cylinder in a turbulent cross flow.

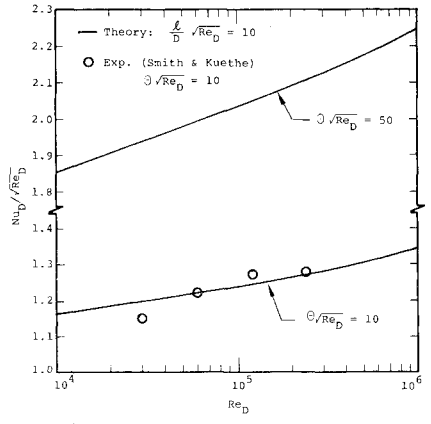

Fig. 5 Effect of Reynolds number on stagnation-point heat transfer for a cylinder in a turbulent cross flow.

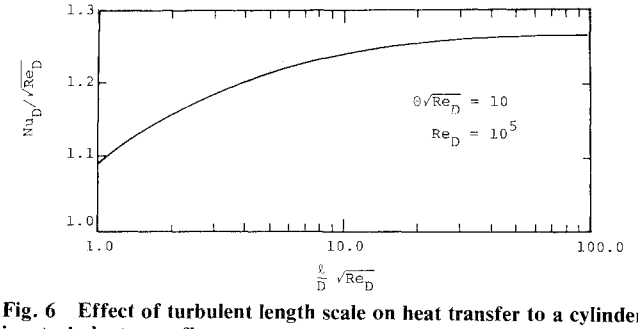

Fig. 6 Effect of turbulent length scale on heat transfer to a cylinder in a turbulent cross flow.

an appropriate value for comparison to at least the Smith and Kuethe data.

The only block of data which is inconsistent with the present theory is that due to Kestin[6](Fig. 4). The reported test conditions indicate that these data should compare to data found by the other investigators. No manner of variation of turbulent-length-scale parameter or Reynolds number could bring the data into agreement with the theoretical predictions given here so that, if correct, the peculiar trend of the Kestin data must remain unexplained.

Present results indicate Fig. 4's moderate data scatter is due to variations in Reynolds number and turbulent length scale

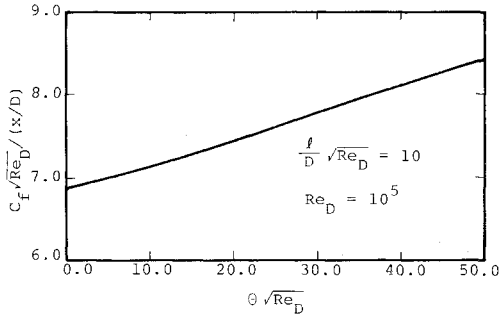

Fig. 7 Stagnation-point shear stress coefficient for a cylinder in a turbulent cross flow.

over and above normal experimental scatter. This is based on the theoretical examination of Reynolds-number and length-scale effects shown in Figs. 5 and 6, respectively. Figure 5 shows predicted effect of Reynolds number on heat transfer for $(\ell/D)(Re_D)^{1/2} = 10$ and $\Theta(Re_D)^{1/2} = 10$ and 50. As indicated, the theory predicts a modest 20% increase in Froessling number $[Nu_D/(Re_D)^{1/2}]$ for an increase in Reynolds number from 10^4 to 10^6. Of most importance is the close quantitative agreement, shown in Fig. 5, between the theory and the experimental results of Smith and Kuethe for the effect of Reynolds number at a turbulence intensity of Θ $(Re_D)^{1/2} = 10$; specifically, computed and measured Froessling numbers differ by less than 10%. The data indicate a more rapid decrease in low Reynolds numbers limit ($Re_D < 10^5$). However, this slight discrepancy in trend probably is due to the effect of the turbulence scale parameter, $(\ell/D)(Re_D)^{1/2}$. This parameter is taken as constant on the theoretical curve but varies in the range $5 < (\ell/D)(Re_D)^{1/2} < 10$ for the Smith and Kuethe data. As shown in Fig. 6, the turbulence scale parameter, in this range, has a moderate effect on the Froessling number. Moreover, the length-scale effect is in such a direction that it would tend to reduce the discrepancy between theory and experiment for the low Reynolds number ($Re_D = 30{,}000$) data point in Fig. 5.

With regard to the length-scale effect, note that the present theory predicts (Fig. 6) a very weak increase in Froessling number of values of $(\ell/D)(Re_D)^{1/2} < 10$. This does not mean, however, that this trend continues for very-large-scale turbulence, since the turbulence model cannot be expected to apply in this limit. In fact, in the limit of very-large-scale turbulence ($\ell/D \to \infty$), the stagnation-point heat transfer should

approach the laminar value since in this limit the turbulence can be viewed as a slowly varying perturbation to the freestream velocity. Experimental data for the effect of large-scale turbulence on the overall heat transfer to a cylinder,[6] suggests that this indeed is the case.

Shear stress is another interesting quantity near the stagnation point. Figure 7 presents the predicted shear-stress coefficient for $(\ell/D)(Re_D)^{1/2}=10$ and $Re_D=10^5$. As shown, the present analysis predicts a relatively modest increase in shear stress due to freestream turbulence. The result presented here of a somewhat smaller effect of freestream turbulence on skin friction as compared to heat transfer is consistent with the semiempirical analysis of Smith and Kuethe[7] and the vorticity amplification model of Sutera.[14]

IV. Conclusions

Results presented in the preceding sections show that most of the important effects of freestream turbulence on low-speed stagnation-point flow can be accurately predicted with the Saffman turbulence model. The theory is sufficiently general to account for effects of turbulence intensity [$\Theta(Re_D)^{1/2}$], turbulence scale $(\ell/D)(Re_D)^{1/2}$, and Reynolds number (Re_D). Excellent quantitative agreement has been obtained between predicted and measured heat transfer for a wide range of turbulence intensities and Reynolds numbers. A moderate effect of turbulence scale on heat transfer is predicted; however, substantiating experimental data are not available.

One aspect of the present analysis which also has been noted by Sadeh et al.[15] is the importance of the inviscid straining region (Region 2) on the freestream turbulence. The turbulence will undergo significant changes in this region in both intensity and scale; the precise magnitude of the changes is predicted to be strongly affected by Reynolds number.

Based on the success achieved in the present study, further developmental effort would appear to be warranted. Application to supersonic stagnation-point flow can be made in a straightforward manner with proper interpretation of η_∞ and the inviscid mean flow, suitable freestream boundary conditions for e and ω, and the compressible version of the model equations.[18,19] Freestream turbulence-induced mass-transfer augmentation could be analyzed for stagnation-point flow by interpreting Eq. (20) as a species equation, replacing the Prandtl numbers by Schmidt numbers, and specifying suitable surface boundary conditions. Surface roughness effects can be treated through a dissipation-rate boundary condition at the surface analogous to the Saffman-Wilcox[19] approach for fully turbulent boundary layer. The solution method is also amenable to treatment of two-phase stagnation point flow.

References

[1] Schlichting, H., *Boundary Layer Theory,* translated by J. Kestin, McGraw-Hill, New York, 1966.

[2] Froessling, N., *Beitr Geophysik,* Vol. 52, 1938, p. 170.

[3] Squire, H.B., *Modern Developments in Fluid Dynamics,* edited by S. Goldstein, Oxford, Vol. II, 1938, p. 623.

[4] Fay, J.A. and Riddell, R.F., "Theory of Stagnation Point Transfer in Dissociated Air," *Journal of the Aeronautical Sciences,* Vol. 25, Feb. 1958.

[5] Kestin, J., "The Effect of Freestream Turbulence on Heat Rates," *Advances in Heat Transfer,* Vol. 3, Academic Press, New York, 1966, pp. 1-32.

[6] Kestin, J. and Maeder, P.F., "Influence of Turbulence on Transfer of Heat from Cylinders," TN 4018, 1954, NACA.

[7] Smith, M.C. and Kuethe, A.M., "Effects of Turbulence on Laminar Skin Friction and Heat Transfer," *The Physics of Fluids,* Vol. 9, Dec. 1966, pp. 2337-2344.

[8] Zapp, G.M., M.S.E. thesis, 1950, Oregon State University, Corvallis, Ore.

[9] Lighthill, M.J., "Contributions to the Theory of Heat Transfer through a Laminar Boundary Layer," *Proceedings of the Royal Society of London,* Vol. A202, 1950, p. 359.

[10] Lin, C.C., *Proceedings of the Ninth International Congress on Applied Mechanics,* Univ. of Brussels, Brussels, Belgium, 1957.

[11] Glauert, M.B., *Journal of Fluid Mechanics,* Vol. 1, 1956, p. 97.

[12] Ishigaki, H., "Heat Transfer in a Periodic Boundary Layer near a Two-Dimensional Stagnation Point," *Journal of Fluid Mechanics,* Vol. 56, Pt. 4, 1972, pp. 619-627.

[13] Sutera, S.P., Maeder, P.F., and Kestin, J., *Journal of Fluid Mechanics,* Vol. 16, 1963, p. 497.

[14] Sutera, S.P., *Journal of Fluid Mechanics,* Vol. 21, 1965, p. 513.

[15] Sadeh, W.Z., Sutera, S.P., and Maeder, P.F., "Analysis of Vorticity Amplification in the Flow Approaching a Two-Dimensional Stagnation Point," *Zeitschrift fuer Angewandte Mathematik und Physik,* Vol. 21, 1970, pp. 699-716.

[16] Sadeh, W.Z., Sutera, S.P., and Maeder, P.F., "An Investigation of Vorticity Amplification in Stagnation Point Flow," *Zeitschrift fuer Angewandte Mathematik and Physik,* Vol. 21, 1970, pp. 717-742.

[17] Saffman, P.G., "A Model for Inhomogeneous Turbulent Flows," *Proceedings of the Royal Society of London,* Vol. A317, 1970, p. 417.

[18] Wilcox, D.C. and Alber, I.E., "A Turbulence Model for High Speed Flows," *Proceedings of the 1972 Heat Transfer and Fluid Mechanics Institute,* Stanford Univ. Press, 1972, pp. 231-252.

[19] Saffman, P.G. and Wilcox, D.C., "Turbulence Model Predictions for Turbulent Boundary Layers," *AIAA Journal,* Vol. 12, April 1974, pp. 541-546.

[20] Wilcox, D.C., "Calculation of Turbulent Boundary-Layer Shock-Wave Interaction," *AIAA Journal,* Vol. 11, Nov. 1973, pp. 1592-1594.

[21] Wilcox, D.C., "Turbulence Model Calculations of Rayleigh Shear Flow," Tech. Rept. DCW-R-NC-01, April 1974, DCW Industries, Sherman Oaks, Calif.

[22] Bearman, P.W., "Some Measurements of the Distortion of Turbulence Approaching a Two-Dimensional Bluff Body," *Journal of Fluid Mechanics,* Vol. 53, Pt. 3, 1972.